Electronic Supplementary Material (ESI) for ChemComm.

Supporting information for: Collision Cross Section Predictions using 2-Dimensional Molecular Descriptors, by Soper-Hopper *et al.*

Corresponding author: Facundo M. Fernandez

E-mail: facundo.fernandez@chemistry.gatech.edu

Ph: 404 385 4432

Fax: 404 385 6447

General Workflow.

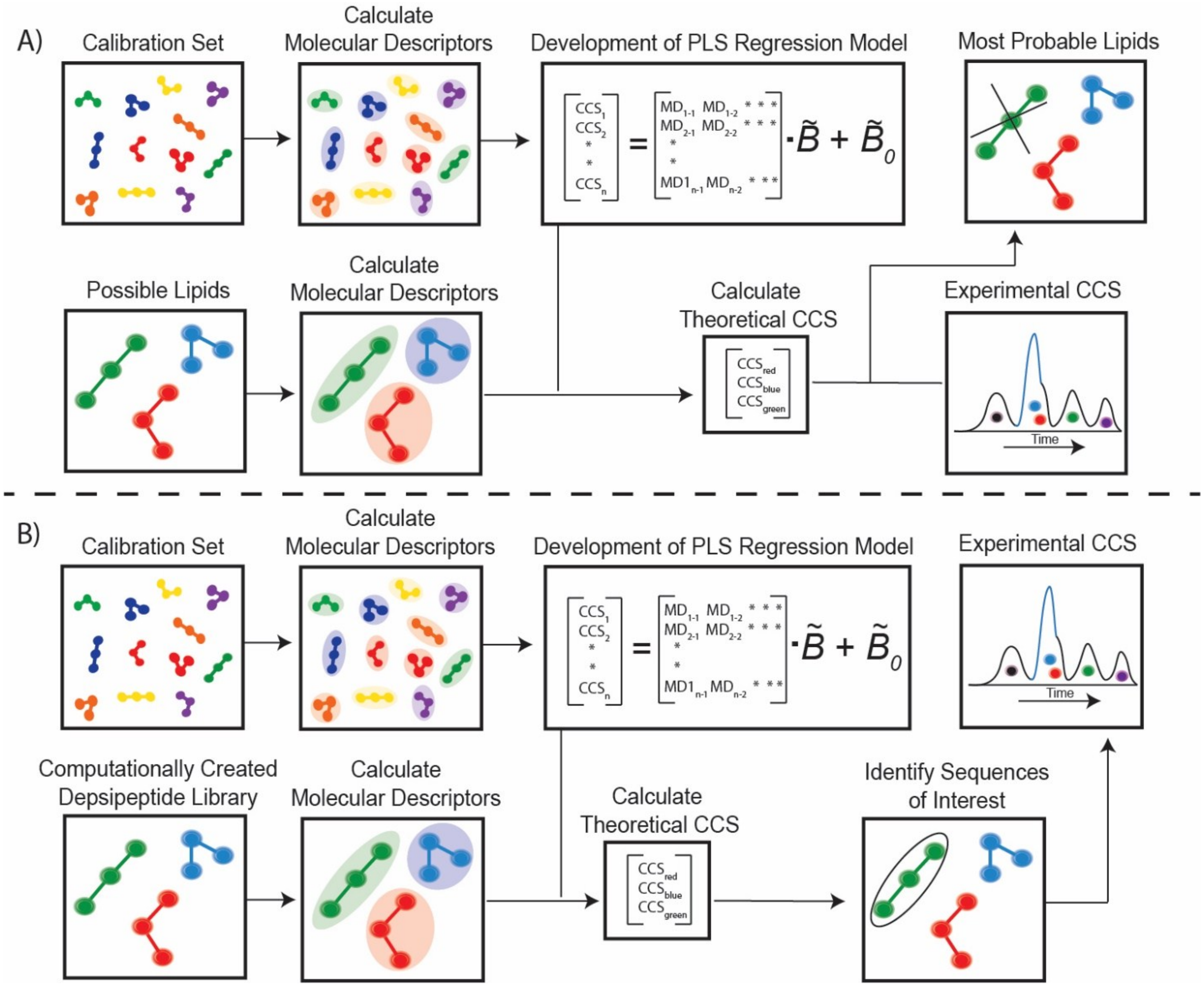
A)
Calibration Set
Calculate Molecular Descriptors
Development of PLS Regression Model
CCS_1 CCS_2 * * CCS_n = MD_{1-1} MD_{1-2} * * * MD_{2-1} MD_{2-2} * * * * * $MD1_{n-1}$ MD_{n-2} * * * $\cdot\tilde{B} + \tilde{B}_0$
Most Probable Lipids
Possible Lipids
Calculate Molecular Descriptors
Calculate Theoretical CCS
CCS_{red} CCS_{blue} CCS_{green}
Experimental CCS
Time
B)
Calibration Set
Calculate Molecular Descriptors
Development of PLS Regression Model
Experimental CCS
Time
Computationally Created Depsipeptide Library
Calculate Molecular Descriptors
Calculate Theoretical CCS
CCS_{red} CCS_{blue} CCS_{green}
Identify Sequences of Interest

Collision cross section prediction can be applied to many areas of research. Highlighted here are two such applications. In A) the molecular descriptors for a a calibration set of lipids with known CCS are used to develop a PLS regression model. The PLS model can then be used to calculate the theoretical CCS of a pool of new lipids which have been selected by MS and MS/MS. The theoretical CCS value is compared to the experimentally measured CCS to narrow down the pool of potential lipids for a more accurate identification. In the other scenario, B), a calibration set made up of pure amino acid chains and pure hydroxy acid chains are used in the development of the PLS regression model. This model is then applied to a library of depsipeptides composed of the amino acids and hydroxy acids used in the calibration. This library is built computationally and consists of all possible combinations of monomeric units, up to a specified chain length. Theoretical CCS values are compared to one another to identify sequences which deviate significantly from the norm. These sequences can then be subjected to experiments such as IM-MS, circular dichroism, NMR, microscopy, and other structural biology techniques.

Lipid CCS prediction model development.

The accompanying spread sheet details the calibration and validation sets for the lipid model development. Collision cross section (CCS) values were taken from the Astarita *et. al.* database[1]. General classes of lipids used are shown below.

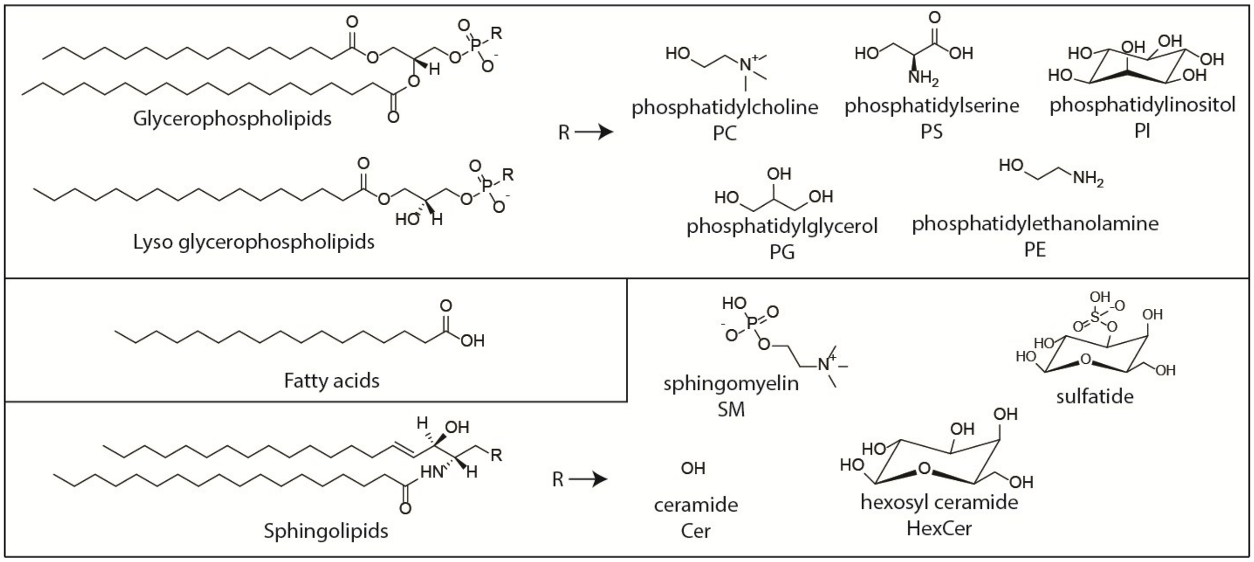

Results of PLS model using all molecular descriptors (excluding 3D descriptors) for lipids are detailed below.

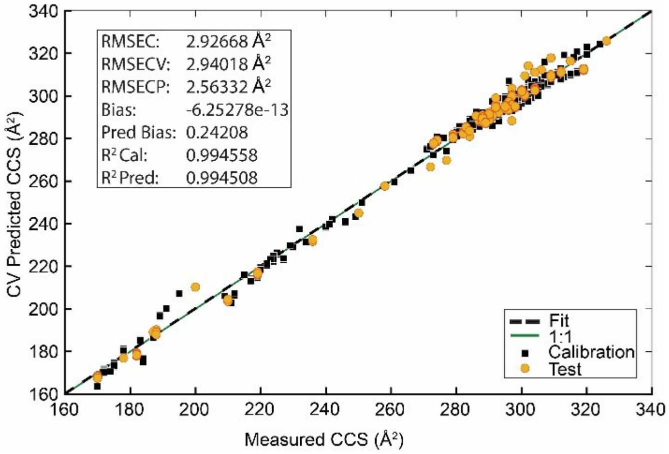

Genetic algorithms and reverse iPLS were used to reduce the total number of molecular descriptors from 3827 to 68. Genetic algorithms with population sizes of 124-256, a window width of 1, and penalty slope of 0.01 were tested. A maximum of 25 variables (descriptors) was targeted over a maximum of 200 generations with 50% variable overlap at convergence, and a mutation rate of 0.003-0.007 (double crossover). Random block cross validation was employed on 5 splits and 5 iterations. The overall GA runs were replicated 3 times. The table below details the parameters used for each GA and the total number of selected molecular descriptors in each GA. The selected molecular descriptors were pooled, and further reduced by reverse iPLS. Unless specified the parameters in the table are the same as Set A.

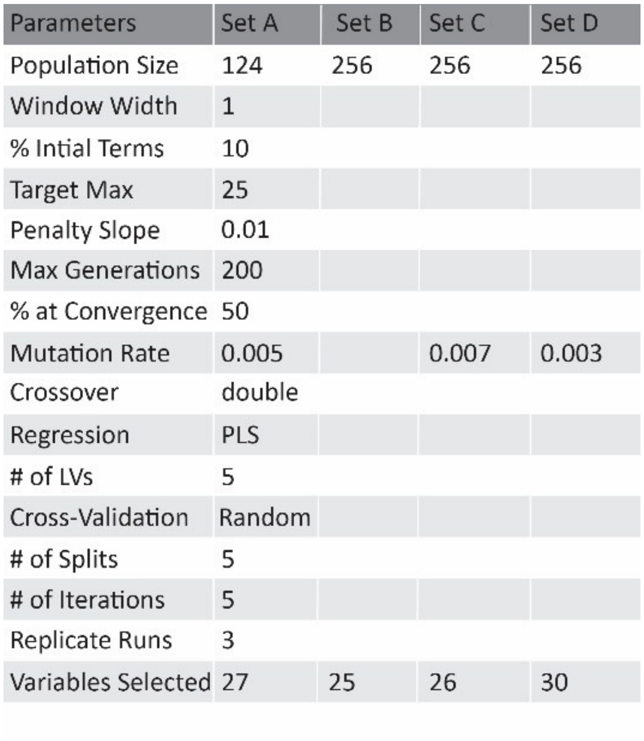

Parameters	Set A	Set B	Set C	Set D
Population Size	124	256	256	256
Window Width	1			
% Intial Terms	10			
Target Max	25			
Penalty Slope	0.01			
Max Generations	200			
% at Convergence	50			
Mutation Rate	0.005		0.007	0.003
Crossover	double			
Regression	PLS			
# of LVs	5			
Cross-Validation	Random			
# of Splits	5			
# of Iterations	5			
Replicate Runs	3			
Variables Selected	27	25	26	30

The final molecular descriptors selected for lipid CCS prediction are listed below with their variable importance in projection (VIP) score. The higher the score, the more influential the molecular descriptor is to the final model. A VIP score close to or greater than one indicates the a variable important to the model. The molecular descriptor with the highest VIP score was Information Index on Molecular Size (ISIZ). Each molecular descriptor belongs to a class of descriptor. The descriptors with highest VIP scores typically fall into 4 main categories: information indices, 2D-Matrix based descriptors, burden eigenvalues, and topological indices.

Name	Description	VIP Score
ISIZ	information index on molecular size	1.707809
Ho_Dz(Z)	Hosoya-like index (log function) from Barysz matrix weighted by atomic number	1.683778
SpMax_D/Dt	leading eigenvalue from distance/detour matrix	1.678203
Ho_D	Hosoya-like index (log function) from topological distance matrix	1.670958
SpDiam_Dz(e)	spectral diameter from Barysz matrix weighted by Sanderson electronegativity	1.657083
SpMin6_Bh(i)	smallest eigenvalue n. 6 of Burden matrix weighted by ionization potential	1.640293
SpMin5_Bh(i)	smallest eigenvalue n. 5 of Burden matrix weighted by ionization potential	1.639537
Wi_D/Dt	Wiener-like index from distance/detour matrix	1.632239
VE2_Dz(v)	average coefficient of the last eigenvector (absolute values) from Barysz matrix weighted by van der Waals volume	1.631325

VE2_D	average coefficient of the last eigenvector (absolute values) from topological distance matrix	1.629118
BAC	Balaban centric index	1.628818
VE2_Dz(i)	average coefficient of the last eigenvector (absolute values) from Barysz matrix weighted by ionization potential	1.624038
SpMAD_D/Dt	spectral mean absolute deviation from distance/detour matrix	1.600553
IDET	total information content on the distance equality	1.595744
ATS3m	Broto-Moreau autocorrelation of lag 3 (log function) weighted by mass	1.586922
Eig12_AEA(dm)	eigenvalue n. 12 from augmented edge adjacency mat. weighted by dipole moment	1.585274
Wi_Dz(i)	Wiener-like index from Barysz matrix weighted by ionization potential	1.580123
Wi_Dz(p)	Wiener-like index from Barysz matrix weighted by polarizability	1.572199
QW_L	quasi-Wiener index (Kirchhoff number) from Laplace matrix	1.562315
SMTI	Schultz Molecular Topological Index (MTI)	1.546356
SM06_AEA(bo)	spectral moment of order 6 from augmented edge adjacency mat. weighted by bond order	1.541396
GMTI	Gutman Molecular Topological Index	1.534685
Eig06_EA(ri)	eigenvalue n. 6 from edge adjacency mat. weighted by resonance integral	1.528521
IDMT	total information content on the distance magnitude	1.527572
H_D/Dt	Harary-like index from distance/detour matrix	1.521057
CENT	centralization	1.520379
SM07_AEA(bo)	spectral moment of order 7 from augmented edge adjacency mat. weighted by bond order	1.517004
SM03_EA(ed)	spectral moment of order 3 from edge adjacency mat. weighted by edge degree	1.453774
nCsp3	number of sp3 hybridized Carbon atoms	1.444398
SM09_EA(ed)	spectral moment of order 9 from edge adjacency mat. weighted by edge degree	1.416581
SpMax3_Bh(v)	largest eigenvalue n. 3 of Burden matrix weighted by van der Waals volume	1.414511
SM12_EA(ed)	spectral moment of order 12 from edge adjacency mat. weighted by edge degree	1.409085
SpMax_L	leading eigenvalue from Laplace matrix	1.393004
Eig04_AEA(bo)	eigenvalue n. 4 from augmented edge adjacency mat. weighted by bond order	1.315147
DECC	eccentric	1.31135
Eig04_EA(bo)	eigenvalue n. 4 from edge adjacency mat. weighted by bond order	1.300912
SpMax_B(m)	leading eigenvalue from Burden matrix weighted by mass	1.251246
C-002	CH2R2	1.140123
ALOGP	Ghose-Crippen octanol-water partition coeff. (logP)	1.053641
GATS2e	Geary autocorrelation of lag 2 weighted by Sanderson electronegativity	1.04824
ALOGP2	squared Ghose-Crippen octanol-water partition coeff. (logP^2	0.991153
P_VSA_s_1	P_VSA-like on I-state, bin 1	0.925566
P_VSA_p_4	P_VSA-like on polarizability, bin 4	0.902342
JGI8	mean topological charge index of order 8	0.710091

SpMax5_Bh(s)	largest eigenvalue n. 5 of Burden matrix weighted by I-state	0.548636
P_VSA_LogP_4	P_VSA-like on LogP, bin 4	0.510328
PW4	path/walk 4 - Randic shape index	0.46771
IC3	Information Content index (neighborhood symmetry of 3-order)	0.388996
Eig03_EA(dm)	eigenvalue n. 3 from edge adjacency mat. weighted by dipole moment	0.369221
CATS2D_00_AN	CATS2D Acceptor-Negative at lag 00	0.229799
CATS2D_05_DL	CATS2D Donor-Lipophilic at lag 05	0.224391
MATS7m	Moran autocorrelation of lag 7 weighted by mass	0.219895
MCD	molecular cyclized degree	0.18916
Chi_D/Dt	Randic-like index from distance/detour matrix	0.185162
WiA_D/Dt	average Wiener-like index from distance/detour matrix	0.185036
Eig08_EA(dm)	eigenvalue n. 8 from edge adjacency mat. weighted by dipole moment	0.13586
MATS6p	Moran autocorrelation of lag 6 weighted by polarizability	0.107775
NssNH	Number of atoms of type ssNH	0.098605
B04[C-N]	Presence/absence of C - N at topological distance 4	0.098605
SIC2	Structural Information Content index (neighborhood symmetry of 2-order)	0.0898
B02[O-O]	Presence/absence of O - O at topological distance 2	0.082945
Eig09_EA(dm)	eigenvalue n. 9 from edge adjacency mat. weighted by dipole moment	0.063465
N-066	Al-NH2	0.057733
SsNH2	Sum of sNH2 E-states	0.057132
VE1sign_D/Dt	coefficient sum of the last eigenvector from distance/detour matrix	0.038758
nOHp	number of primary alcohols	0.021518
VE1sign_D	coefficient sum of the last eigenvector from topological distance matrix	0.005006
SRW03	self-returning walk count of order 3	0

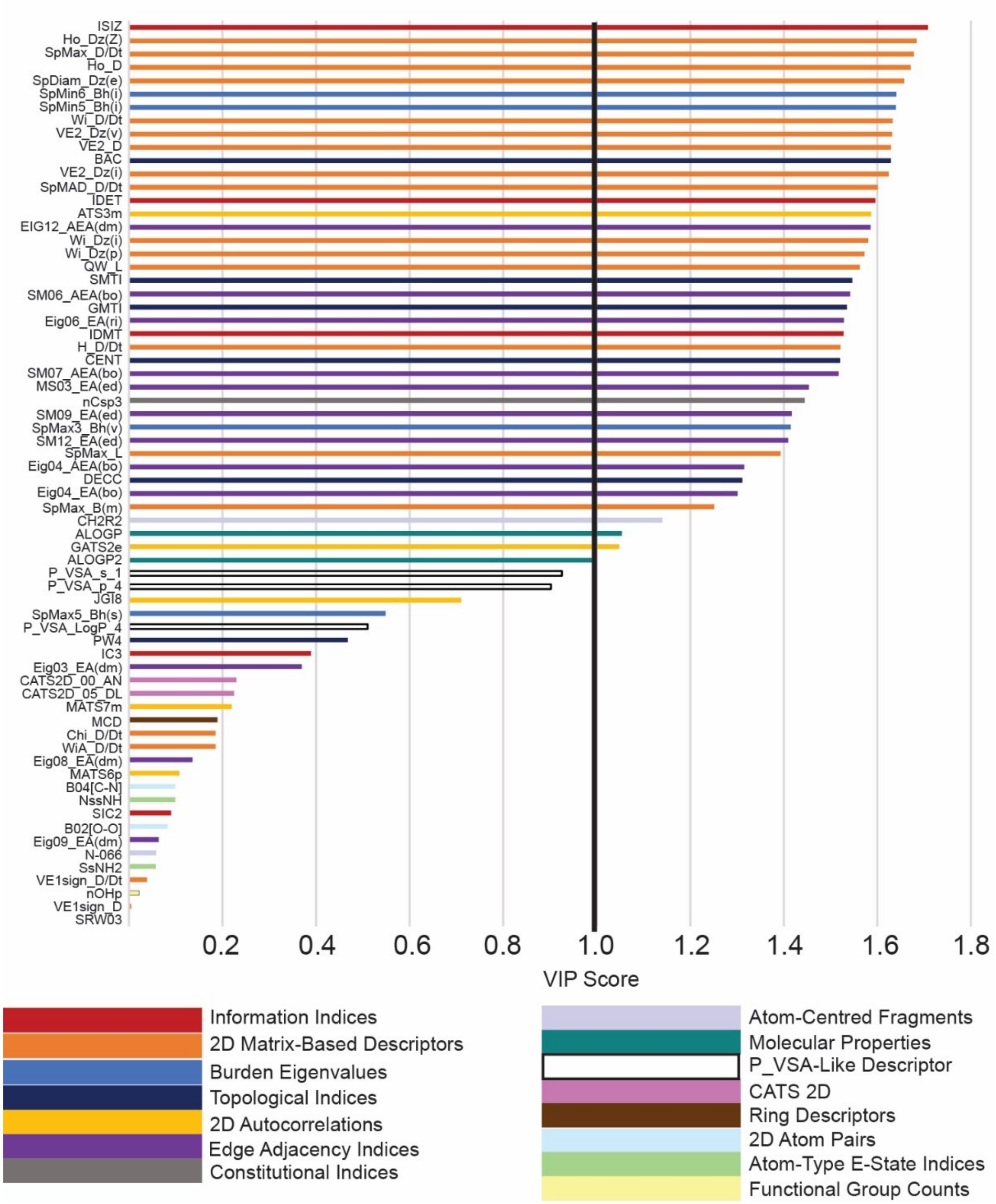

Depsipeptide CCS Prediction

Depsipeptides contain a mixed hydroxy acid/ amino acid backbone. Shown below is the structure for a representative depsipeptide with lactic acid and a generic amino acid. Hydroxy acids are boxed in red, with the amino acids in blue.

Molecular

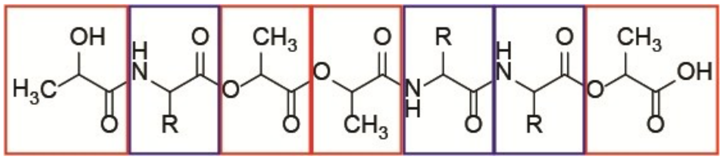

descriptor

calculation for depsipeptides.

Sequence of the depsipeptides of a desired length were generated in FASTA file format via permutations of the alphabet of amino and hydroxy acids of a certain type (alanine and lactic acid for this work), where the capital letters represented amino acids and equivalent small letters denoted the corresponding hydroxy acids. The FASTA sequences were then converted to the 3D structure files in mol2 format using an in house modified OpenBabel package. The resulting mol2 files were uploaded into Dragon 7.0. Molecular descriptors were calculated as the same way detailed for the lipids, and excluding all 3D descriptors.

To enable the support for both hyrdoxy and amino acids, the fastaformat.cpp routine of OpenBabel was modified in two ways. First, a case sensitivity support was added to the code to distinguish between the sets of the amino and hydroxy acids. Second, a new sequence type DepsiSequence containing both hydroxy and amino acid residues was added to the routine. A set of residue record for DepsiResidues was created. The records for the amino acid residues have been copied from the existing ProteinResidues record. The records for the corresponding hydroxy acid residues were generated by editing the records for the amino acid residues and replacing an amide “N” atom with ester “O” and removing the attached hydrogen. The beta strand conformation inherited from the protein residues was retained for all hydroxy acid residues.

Depsipeptide Synthesis. One hundred µL of the sample solution containing 100 mM of L-lactic acid and 100 mM L-alanine was heated to 95^{0}C by a Bio-Rad MyCycler 96 well thermal cycler. The oligomer mixtures were obtained after 3 days dry down. Both L-lactic acid and L-alanine were from Sigma-Aldrich.

IM-MS Instrumental Methods. Mass spectra were collected on a quadrupole-ion mobility-time-of-flight mass spectrometer (Synapt G2 HDMS, Waters, Milford, MA, USA) with an electrospray ionization source. Depsipeptide ions were generated using direct infusion at a capillary voltage of 2.5kV. The source was operated in negative ion mode with a source temperature of 80°C, the sample cone at 30 V and extraction cone at 3.0 V. The desolvation gas flow was 650 L/Hr, and a desolvation temperature of 250°C. The trap region of the traveling wave IM separator was operated at a wave velocity of 311 m/s, wave height of 6.0 V. The IMS wave velocity was 500 m/s, with a wave height of 40 V. The transfer wave velocity was 190 m/s, with a wave height of 4.0 V. Fragmentation was induced in the transfer region using a transfer collision energy between 10 and 40V. Mass spectra were calibrated using sodium formate and analyzed using MassLynx 4.1 and Driftscope 2.0 software. CCS (Ω) measurements were externally calibrated using the published values for malic acid in nitrogen. Measurements were taken in triplicate. Samples were prepared by rehydrating dried sample in water containing 0.1% formic acid, and analyzed immediately.

MS/MS depsipeptide identification. The quadrupole settings required to achieve a high-enough level of sensitivity for detection did not provide perfect isolation of a single mass. Data shown below shows other species differing by only 1 Da. From previous work, we know that the first residue on the N-terminus of the depsipeptide is a hydroxy acid (for this work, lactic acid). Therefore, we only considered fragments which started with lactic acid. Additionally, we do not typically see b ions in the fragmentation patterns, as the charge carrier is the carboxylic acid at the C-terminus.

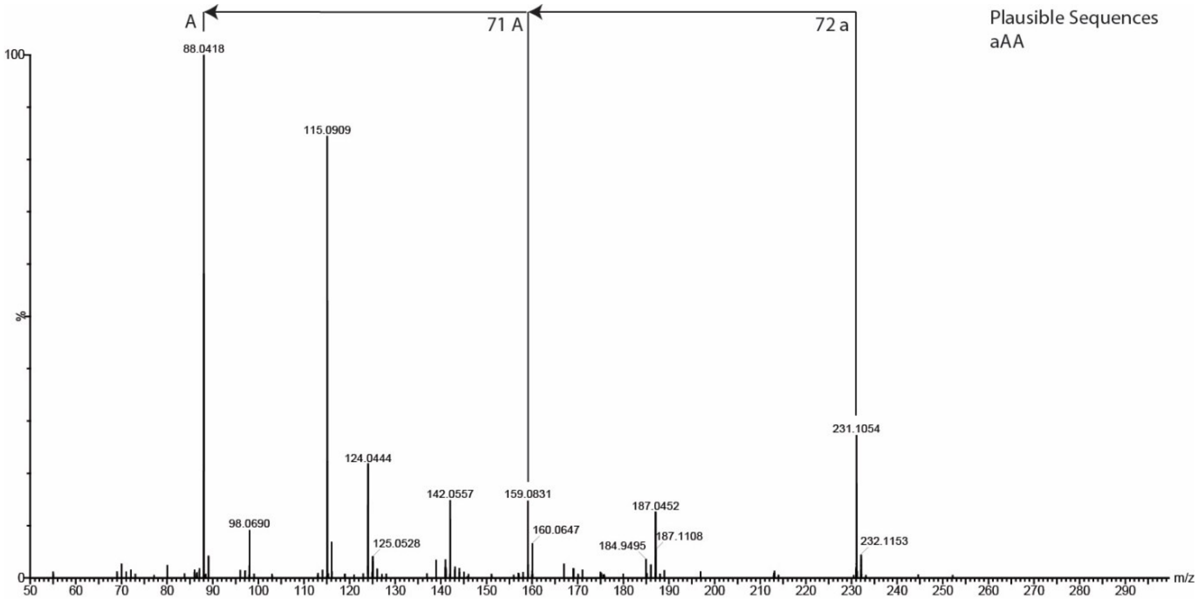

Precursor m/z = 231.105. Isomers contain 1 lactic acid and 2 alanine.

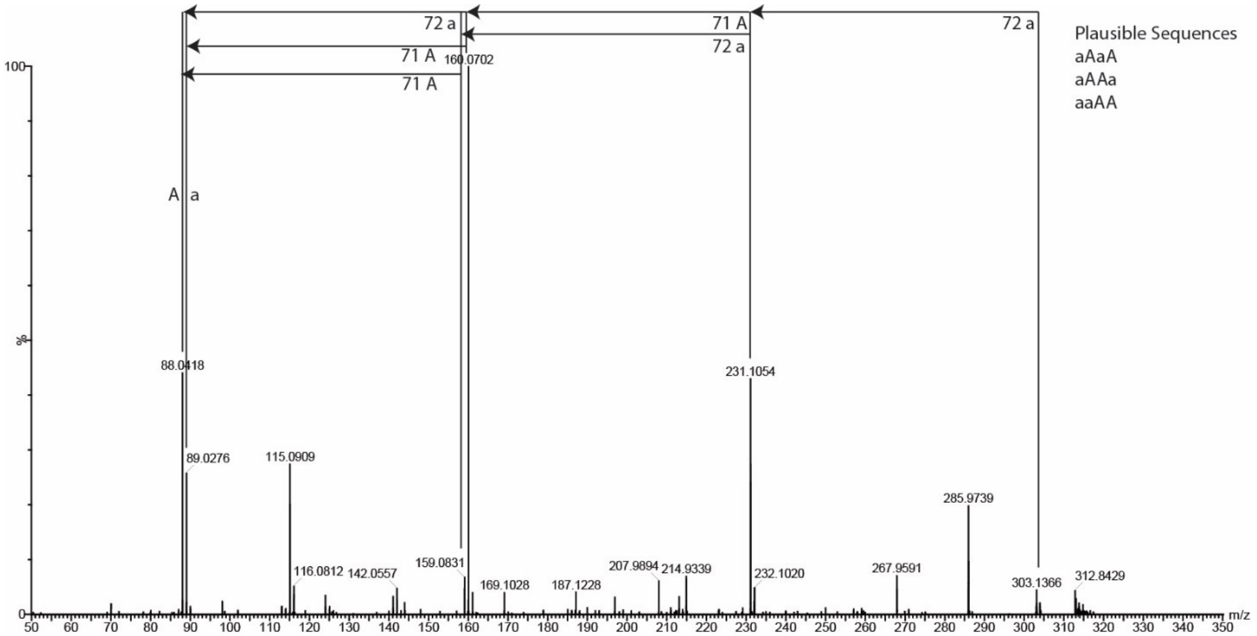

Precursor m/z = 303.137. Isomers contain 2 lactic acid and 2 alanine.

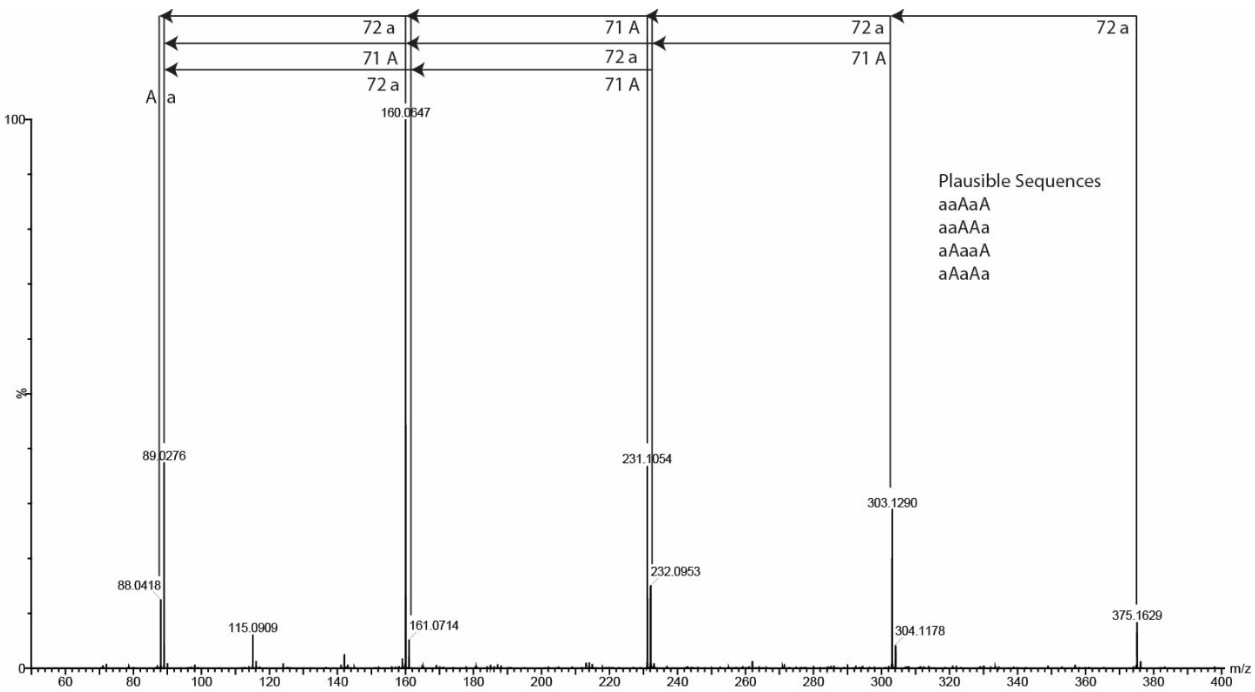

Precursor m/z = 375.163. Isomers contain 3 lactic acid and 2 alanine.

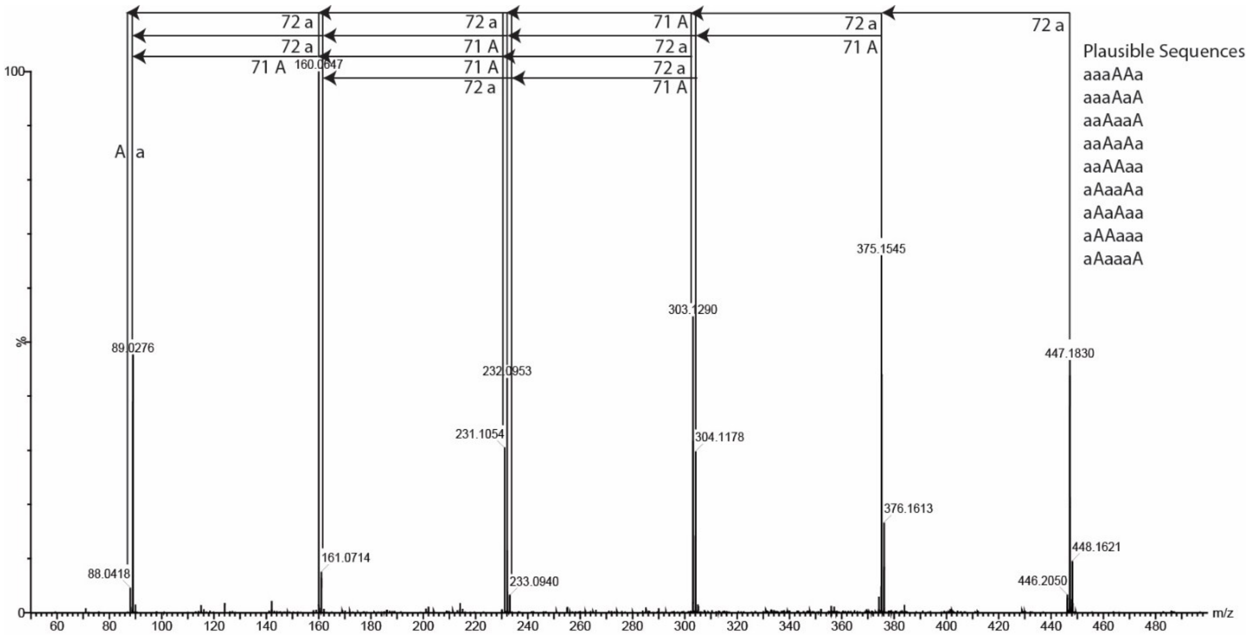

Precursor m/z = 447.183. Isomers contain 4 lactic acid and 2 alanine.

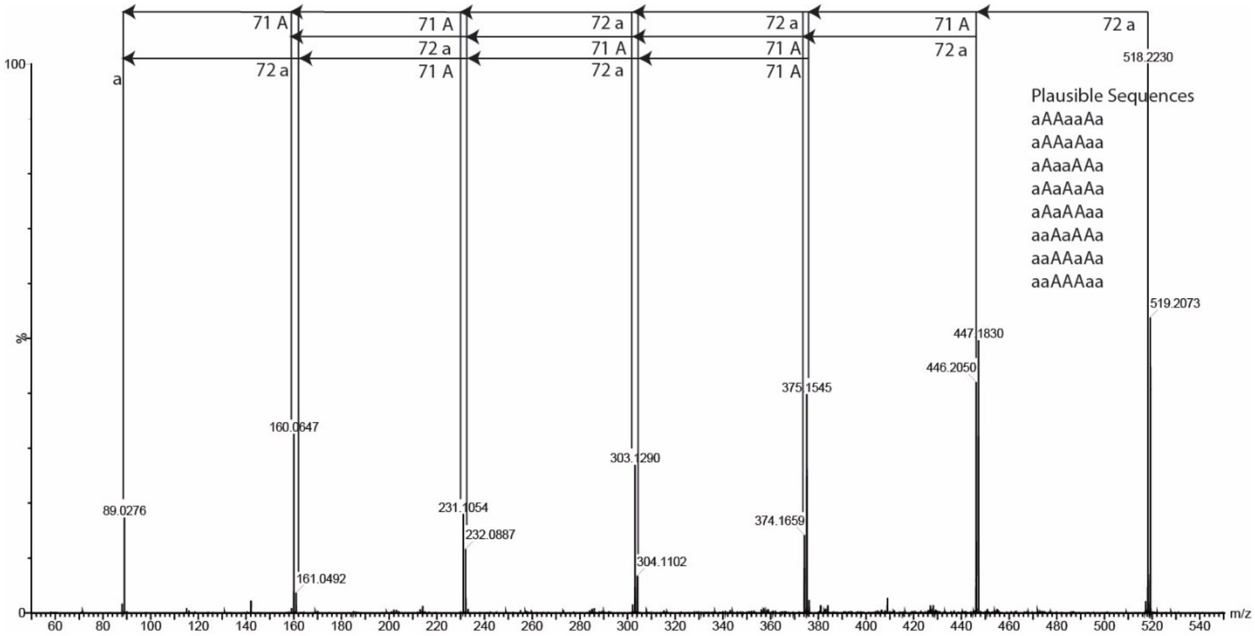

Precursor m/z = 518.223. Isomers contain 4 lactic acid and 3 alanine.

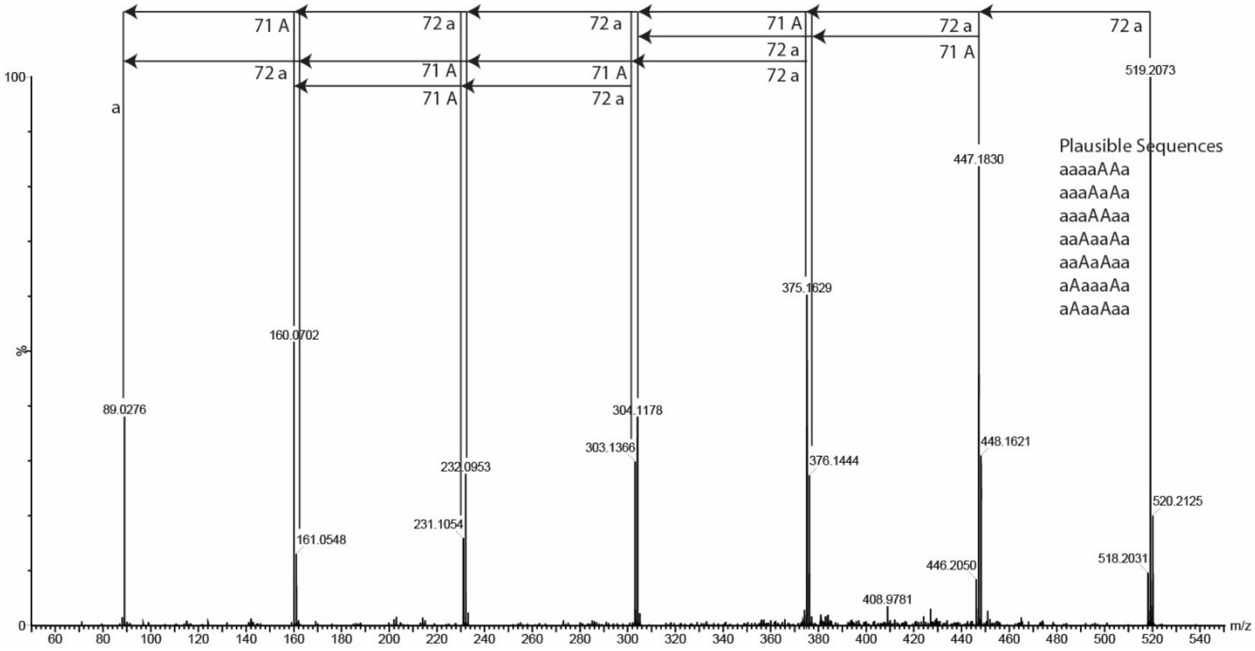

Precursor m/z = 519.207. Isomers contain 5 lactic acid and 2 alanine.

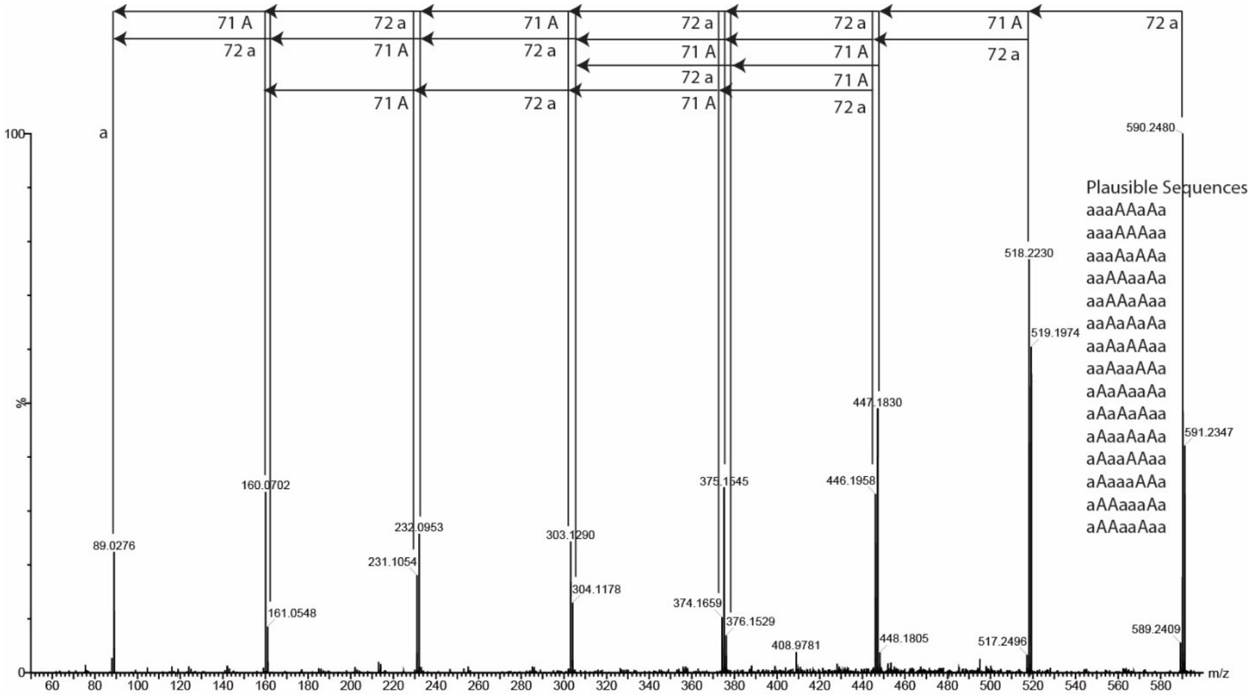

Precursor m/z = 590.248. Isomers contain 5 lactic acid and 3 alanine.

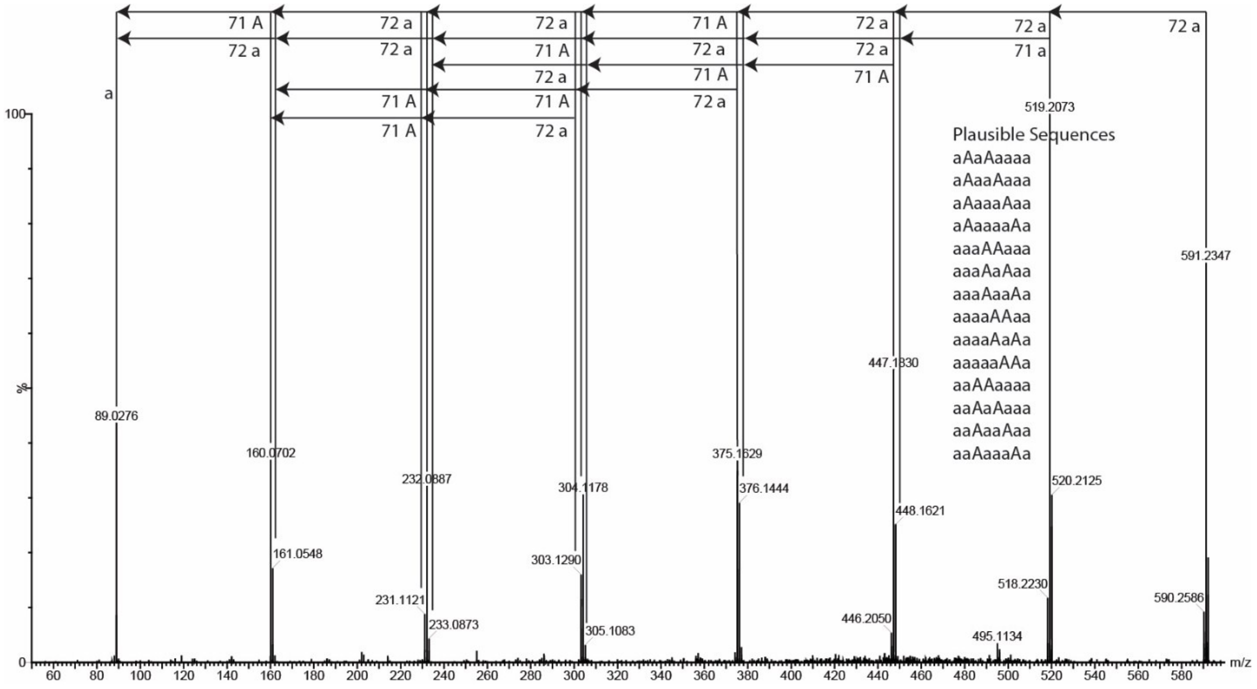

Precursor m/z = 591235. Isomers contain 6 lactic acid and 2 alanine.

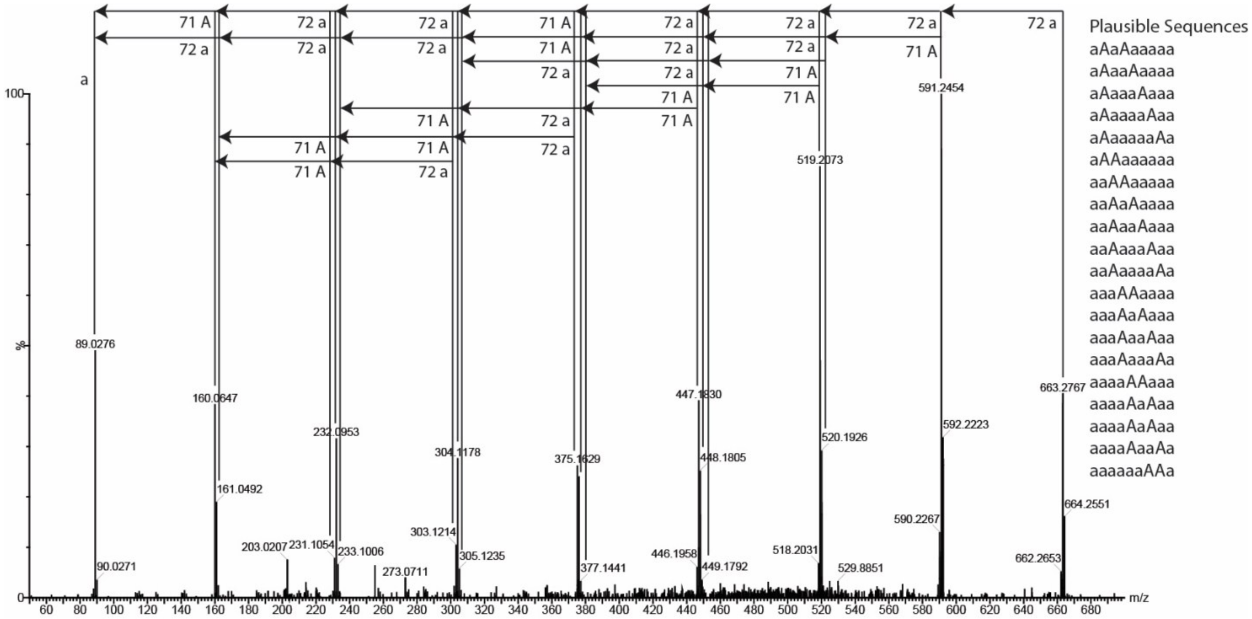

Precursor m/z = 633.277. Isomers contain 7 lactic acid and 2 alanine.

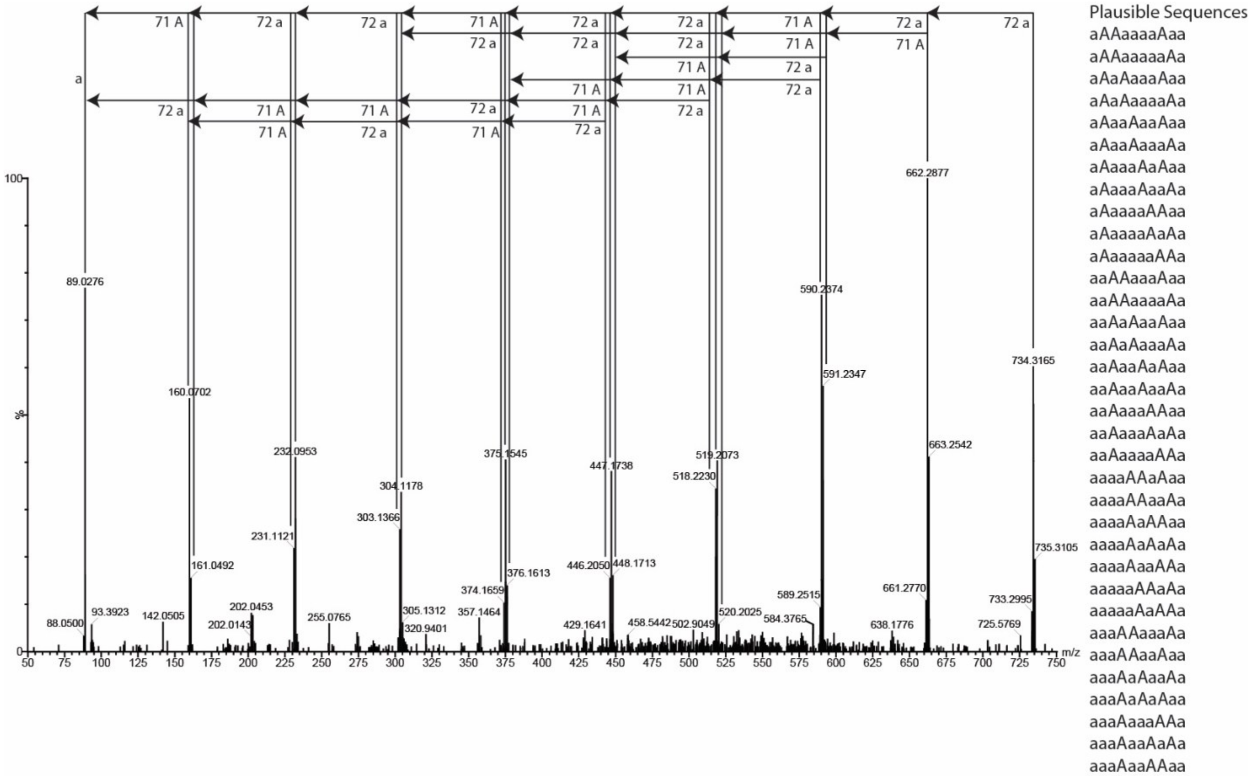

Precursor m/z = 734.317. Isomers contain 7 lactic acid and 3 alanine.

We checked the accuracy of our predictions through comparison to the sequenced fragments. Below is a table of the % difference for each sequence identified. The percent difference is always less than 3%, within the experimental error of IM-MS instruments.

Sequence	Predicted CCS (Å²)	Measured CCS (Å²)	% Difference
aAA	149.54	150.01	-0.32
aAaA	165.27	167.23	-1.17
aAAa	163.45	167.23	-2.29
aaAA	166.52	167.23	-0.42
aaAaA	180.19	181.05	-0.48
aaAAa	179.63	181.05	-0.79
aAaaA	179.62	181.05	-0.79
aAaAa	178.94	181.05	-1.18
aaaAAa	196.89	195.99	0.46
aaaAaA	196.98	195.99	0.50
aaAaaA	195.93	195.99	-0.03
aaAaAa	195.87	195.99	-0.06
aaAAaa	194.62	195.99	-0.70
aAaaAa	195.75	195.99	-0.12
aAaAaa	194.57	195.99	-0.73
aAAaaa	193.43	195.99	-1.32
aAaaaA	196.08	195.99	0.04
aAAaaAa	208.32	210.01	-0.81
aAAaAaa	207.65	210.01	-1.13
aAaaAAa	210.20	210.01	0.09
aAaAaAa	208.91	210.01	-0.53
aAaAAaa	208.33	210.01	-0.81
aaAaAAa	210.08	210.01	0.03
aaAAaAa	208.72	210.01	-0.62
aaAAAaa	208.03	210.01	-0.95
aaaaAAa	211.27	210.00	0.60
aaaAaAa	210.03	210.00	0.01
aaaAAaa	209.71	210.00	-0.14
aaAaaAa	209.58	210.00	-0.20
aaAaAaa	208.64	210.00	-0.65
aAaaaAa	209.93	210.00	-0.03
aAaaAaa	209.39	210.00	-0.29
aaaAAaAa	224.19	223.25	0.42
aaaAAAaa	224.14	223.25	0.40
aaaAaAAa	225.19	223.25	0.87
aaAAaaAa	222.87	223.25	-0.17
aaAAaAaa	222.73	223.25	-0.23
aaAaAaAa	223.90	223.25	0.29
aaAaAAaa	223.51	223.25	0.12
aaAaaAAa	224.75	223.25	0.67
aAaAaaAa	223.90	223.25	0.29
aAaAaAaa	222.95	223.25	-0.13

Sequence	Predicted CCS (Å^2)	Measured CCS (Å^2)	% Difference
aAaaAaAa	224.38	223.25	0.50
aAaaAAaa	224.13	223.25	0.39
aAaaaAAa	225.19	223.25	0.86
aAAaaaAa	223.01	223.25	-0.11
aAAaaAaa	223.07	223.25	-0.08
aAaAaaaa	222.22	223.24	-0.46
aAaaAaaa	223.14	223.24	-0.05
aAaaaAaa	224.22	223.24	0.44
aAaaaaAa	224.52	223.24	0.57
aaaAAaaa	237.26	223.24	6.09
aaaAaAaa	238.23	223.24	6.50
aaaAaaAa	238.87	223.24	6.76
aaaaAAaa	225.01	223.24	0.79
aaaaAaAa	225.37	223.24	0.95
aaaaaAAa	226.03	223.24	1.24
aaAAaaaa	221.99	223.24	-0.56
aaAaAaaa	222.77	223.24	-0.21
aaAaaAaa	223.97	223.24	0.33
aaAaaaAa	224.17	223.24	0.41
aAaAaaaaa	236.14	237.13	-0.42
aAaaAaaaa	236.78	237.13	-0.15
aAaaaAaaa	237.63	237.13	0.21
aAaaaaAaa	238.89	237.13	0.74
aAaaaaaAa	238.45	237.13	0.56
aAAaaaaaa	236.44	237.13	-0.29
aaAAaaaaa	236.07	237.13	-0.45
aaAaAaaaa	236.02	237.13	-0.47
aaAaaAaaa	237.31	237.13	0.08
aaAaaaAaa	237.83	237.13	0.29
aaAaaaaAa	238.15	237.13	0.43
aaaAAaaaa	236.82	237.13	-0.13
aaaAaAaaa	237.10	237.13	-0.01
aaaAaaAaa	238.32	237.13	0.50
aaaAaaaAa	238.23	237.13	0.47
aaaaAAaaa	238.23	237.13	0.46
aaaaAaAaa	238.37	237.13	0.52
aaaaAaaAa	238.83	237.13	0.72
aaaaaaAAa	240.04	237.13	1.22
aAAaaaaAaa	251.02	249.09	0.77
aAAaaaaaAa	250.56	249.09	0.59
aAaAaaaAaa	250.31	249.09	0.49
aAaAaaaaAa	250.66	249.09	0.63

Sequence	Predicted CCS (Å^2)	Measured CCS (Å^2)	% Difference
aAaaAaaAaa	251.27	249.09	0.87
aAaaAaaaAa	251.00	249.09	0.76
aAaaaAaAaa	251.57	249.09	0.99
aAaaaAaaAa	252.08	249.09	1.19
aAaaaaAAaa	252.36	249.09	1.30
aAaaaaAaAa	252.08	249.09	1.19
aAaaaaaAAa	252.58	249.09	1.39
aaAAaaaAaa	250.24	249.09	0.46
aaAAaaaaAa	249.98	249.09	0.36
aaAaAaaAaa	250.51	249.09	0.57
aaAaAaaaAa	250.13	249.09	0.42
aaAaaAaAaa	251.41	249.09	0.93
aaAaaAaaAa	251.39	249.09	0.92
aaAaaaAAaa	251.92	249.09	1.13
aaAaaaAaAa	251.45	249.09	0.94
aaAaaaaAAa	252.17	249.09	1.23
aaaaAAaAaa	251.77	249.09	1.07
aaaaAAaaAa	251.54	249.09	0.98
aaaaAaAAaa	252.12	249.09	1.21
aaaaAaAaAa	251.70	249.09	1.04
aaaaAaaAAa	252.48	249.09	1.35
aaaaaAAaAa	252.44	249.09	1.34
aaaaaAaAAa	253.13	249.09	1.61
aaaAAaaaAa	250.36	249.09	0.51
aaaAAaaAaa	250.79	249.09	0.68
aaaAaAaaAa	251.21	249.09	0.85
aaaAaAaAaa	250.99	249.09	0.76
aaaAaaaAAa	252.99	249.09	1.55
aaaAaaAaAa	251.68	249.09	1.03
aaaAaaAAaa	252.44	249.09	1.34

CCS Calibration Curve. Below is the calibration curve created for the calculation of experimental CCS measurements on the Waters Synapt G2, operated as described previously. Polymalic acid in negative ion mode was used for calibration[2]. Parameters are as specified above in IM-MS Instrumental Methods.

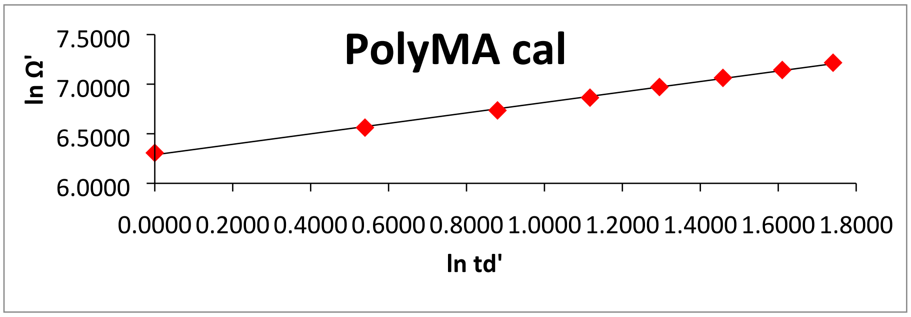

1. G. Paglia, P. Angel, J. P. Williams, K. Richardson, H. J. Olivos, J. W. Thompson, L. Menikarachchi, S. Lai, C. Walsh and A. Moseley, *Analytical chemistry*, 2014, **87**, 1137-1144.
2. J. G. Forsythe, A. S. Petrov, C. A. Walker, S. J. Allen, J. S. Pellissier, M. F. Bush, N. V. Hud and F. M. Fernández, *Analyst*, 2015, **140**, 6853-6861.